NJC

www.rsc.org/njc

LETTER

Macrocyclic ionic liquid crystals†

Lucía Casal-Dujat,[a] Oriol Penon,[a] Carlos Rodríguez-Abreu,[b] Conxita Solans[c] and Lluïsa Pérez-García*[a]

The efficient synthesis of ionic liquid crystals with cationic groups in a cyclophane unit is described, and the striking and complementary roles of the anion and the macrocycle in the mesophase behaviour are demonstrated.

Soft matter systems have properties which depend directly on the topology of the component molecules. In the vast majority of cases, thermotropic liquid crystals (LCs) have a relatively rigid core structure of varying topography and topology which leads to different liquid crystal types and characteristics.[1] Ionic liquid crystals (ILCs)[2] are of particular interest because of the many opportunities they offer, for example as conducting soft materials, chemical solvents or templates, although as a young family of mesogens there lies much to be discovered.

Amongst the different scaffolds employed for the preparation of ILCs, imidazolium moieties are prominent due to the accessible synthetic methodology for their preparation and their structural versatility. Thus, there are many examples of ILCs based on the use of 1,3-dialkylimidazolium salts, with alkyl chains differing in length and rigidity.[3] Also, the use of structures similar to gemini surfactants has been only more recently explored, using either flexible[4a,b] or rigid connectors between the two imidazolium rings,[4c,d] and it seems to offer some clear advantages.

The generally smectic nature of the mesophases—caused by nanophase separation of the charged and lipophilic sections of the molecules—also offers the chance to study the effects of rigidity in the charged end as well as the nature of the anion on the liquid crystalline properties. In this sense, Kouwer and Swager showed recently how a simple linear rigid structure can
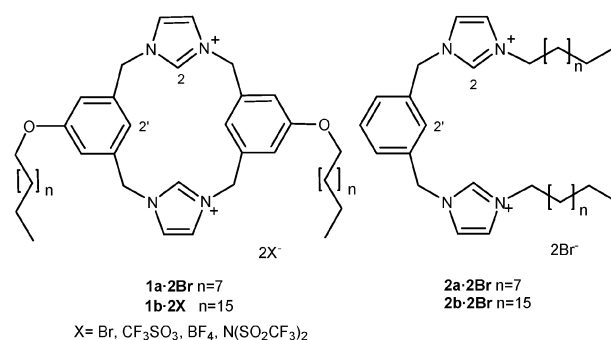
[a] *Department of Pharmacology and Therapeutic Chemistry, Faculty of Pharmacy, and Institute of Nanoscience and Nanotechnology UB (IN2UB), University of Barcelona, 08028, Spain. E-mail: mlperez@ub.edu*
[b] *International Iberian Nanotechnology Laboratory (INL), 4715-330, Braga, Portugal*
[c] *Department of Chemical and Biomolecular Nanotechnology, Institute for Advanced Chemistry of Catalonia, Consejo Superior de Investigaciones Científicas (IQAC/CSIC), 08034, Barcelona, Spain*

† Electronic supplementary information (ESI) available: XRD powder measurement at 25 °C for the cyclophane **1b·2Br** (Fig. S1), XRD powder measurements for **1b·2(N(CF₃SO₂)₂)** with a variation of temperature (Fig. S2a), images obtained by POM-HS of **1b·2(N(CF₃SO₂)₂)** at various temperatures (Fig. S2b), variation in Bragg distances, *d*, in cyclophanes **1·2X** and protophanes **2·2Br** (Table S1), characterization of dicationic macrocycles **1·2X** (experimental). See DOI: 10.1039/c2nj20934a

Fig. 1 The ionic compounds used in this study.

influence both transition temperature and the phase type.[5] On the other hand, the anion is known to play a role in the clearing temperatures and the phase ranges, although there are apparently no standard trends in the materials.[6]

In this work we aimed to study the effect of charged head group topology on the liquid crystal properties of gemini amphiphilic imidazolium based molecules. While ionic liquid crystals have been found for bis-imidazolium compounds with a linear topology,[4] the macrocyclic feature has up to now been unexplored for imidazolium compounds in these materials. We report here the macrocyclic ionic compounds **1** and compare them with the open analogues **2** (Fig. 1), and have found that the macrocycle influences greatly the clearing temperatures of these bis-imidazolium systems. The compounds investigated include (a) dicationic heterophanes **1·2Br** formed by two imidazolium rings linked by a 1,3-dimethylenebenzene spacer, where the benzene rings incorporate long alkyl chains of 10 or 18 carbon atoms, and (b) protoheterophanes **2·2Br**, where the imidazolium rings incorporate the long alkyl chains. The combination of a rigid macrocyclic core structure and a charged component whose phase behaviour can be changed by interchanging anions is a novel aspect of these compounds.

Macrocycles **1·2Br** were obtained in high yield following a "3 + 1" convergent approach (Scheme 1).[7] Thus, bromination of 1,3-bis(hydroxymethyl)-5-alkyloxybenzenes **3a** or **3b**[8] using phosphorous tribromide afforded the corresponding 1,3-bis(bromomethyl)derivatives **4a** or **4b**[9] (>73%), which reacted with imidazole in basic media to yield protophanes **5** (>73%) (Scheme 1). The anion-templated macrocyclization of **5a** or **5b**
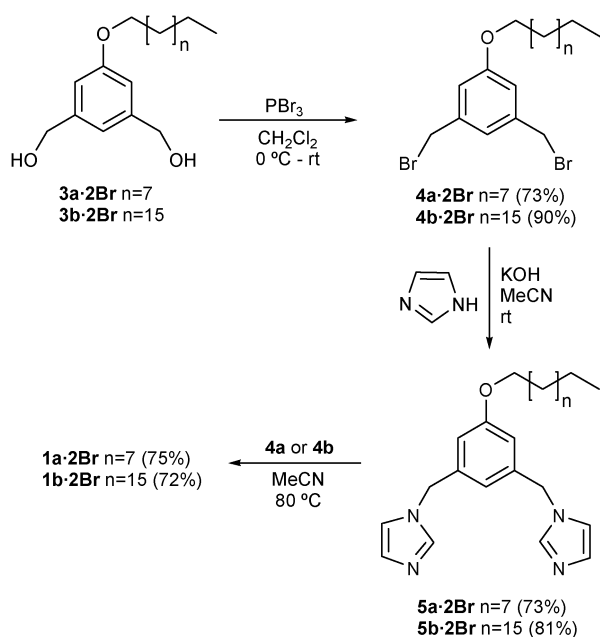
Scheme 1 Synthesis of macrocycles **1b·2Br**.

with **4a** or **4b**, respectively, gave dicationic macrocycles **1·2Br** ($>72\%$), and following an anion exchange protocol in solution, macrocycles **1b·BF₄**, **1b·2CF₃SO₃**, and **1b·2N(CF₃SO₂)₂** were prepared in good yields (*ca.* 60%). The synthesis (90%) of **2a·2Br** was achieved[7] by quaternization of 1,3-bis(imidazolylmethyl)benzene[10] with 1-bromodecane, whereas compound **2b·2Br** was obtained (85%) by quaternization of *N*-octadecyl-1*H*-imidazole[11] with 1,3-bis(bromomethyl)benzene.

The ^{1}H NMR spectra of dications **1·2Br** and **2·2Br** in CDCl₃ showed sharp singlets for the bridging methylene protons, which indicated high conformational mobility as was also observed in previously prepared [14]metaheterophanes and protophanes.[10,12] The ^{1}H NMR chemical shifts in CDCl₃ for the hydrogen atoms in the 2 position of both the imidazolium and the benzene rings are listed in Table 1, for **1b·2X** and **2·2Br**, and give significant structural information. First, it is worth mentioning the solvent effect, since the ^{1}H NMR chemical shifts observed in CDCl₃ for the C(2)–H on the imidazolium ring of compound **1b·2Br** appear 1.71 ppm downfield compared with those observed in (CD₃)₂SO; also, the chemical shifts for the C(2)′–H on the benzene ring are shifted 1.25 ppm upfield in (CD₃)₂SO (Table 1). These observations are the result of the increasing polarity of the solvent and the

Table 1 Selected ^{1}H NMR chemical shifts for compounds **1b·2X** and **2·2Br**

Compound	δ C(2)–H (imidazolium)/ppm	δ C(2)′–H (benzene)/ppm
1b·2Br[a]	10.97	7.82
1b·2Br[b]	9.26	6.57
1b·2CF₃SO₃[a]	9.72	7.01
1b·2BF₄[a]	9.64	7.00
1b·2N(CF₃SO₂)₂[a]	9.14	6.53
2a·2Br[a]	10.43	8.12
2b·2Br[a]	10.41	8.09

[a] In CDCl₃. [b] In (CD₃)₂SO.

diminished hydrogen bonds between the macrocycle and its corresponding anion.

Secondly, the proton chemical shifts shown in Table 1 indicate that the δ values of the acidic C(2)–H imidazolium experiment a deshielding effect due to structural factors and also an anion effect was observed, indicating the acidity of these hydrogen atoms, and therefore, their propensity to metal and anion coordination. It is clear from Table 1 that chemical shifts for compound **1b·2X** are extremely dependent on the counterion. Thus, C(2)–H on the imidazolium ring for **1b·2Br** are the most deshielded hydrogen atoms (Table 1) whereas **1b·2CF₃SO₃**, **1b·2BF₄**, and **1b·2N(CF₃SO₂)₂** exhibit these protons shifted upfield 1.25 ppm, 1.33 ppm and 1.83 ppm, respectively. A similar order for the shielding effect is observed for the C(2)′–H on the benzene ring (Table 1), although their contribution to the anion hydrogen bonding is weaker. These chemical shifts are clearly correlated with the ability of forming weak hydrogen bonds with their corresponding counterions, responsible for their anion binding ability,[10] and their values appear in the order Br ≫ CF₃SO₃ > BF₄ ≫ N(CF₃SO₂)₂, which also has important implications in their supramolecular order and their liquid crystal behaviour (*vide infra*). Finally, ^{1}H NMR chemical shifts for the open chain compounds **2·2Br** seem to indicate a higher interaction with the bromide counterion of the C(2)′–H on the benzene rings, according to their shift downfield in comparison with their corresponding macrocyclic analogues (Table 1), as a result of its open structure compared to the cyclic scaffold whose rigid constitution helps increase complexation with counter-ions.

The thermotropic behaviour of the new compounds was explored by differential scanning calorimetry (DSC), thermogravimetric analysis (TGA), polarized optical microscopy with hot stage (POM-HS) and X-ray diffraction (XRD), and the results obtained are summarized in Table 2. All the compounds studied, **1·2X** and **2·2Br**, displayed thermotropic behaviour, which is influenced by the number of carbon atoms in the alkyl chains, the amphiphilic bis-imidazolium constitution, and the counter-ion.

The number of carbon atoms in the alkyl chains influences the temperatures at which the SC–LC and LC–isotropic liquid transitions occur. Firstly, it has been observed that **2a·2Br** is a LC at room temperature, whereas **2b·2Br** is a crystalline solid at room temperature, with a transition temperature from SC to LC of 60.9 °C (Table 2). Likewise, the clearing point temperatures increase with the length of the hydrophobic tail as **2a·2Br** (57 °C) < **2b·2Br** (250 °C). These facts are probably a consequence of the increase in the van der Waals interactions within the hydrophobic tails, with interdigitation of the chains increasing the interaction and improving the molecular packing.

The cyclophanes **1·2Br** are crystalline solids at room temperature, as shown clearly by the X-ray powder diffractogram (see Fig. S1 in ESI†) where a series of sharp and well-defined reflections are observed. Unlike protophanes, the transition temperatures were higher for the cyclophane incorporating the shorter alkyl chains **1a·2Br** (Table 2). Thus, **1a·2Br** experiences a SC to LC transition at 162.7 °C as shown by DSC (while 107.2 °C for **1b·2Br**), and POM-HS indicated a clearing point at 255 °C (Table 2). Also, both bromide salts of the cyclophanes show solid–solid phase transition prior to LC formation. Again, the bromide interaction

Table 2 Transition temperatures (T_{trans}) and transition enthalpies (ΔH) from DSC thermograms, clearing point temperature (T_{cp}) from POM-HS and decomposition temperature (T_{dec}) from TGA of cyclophanes **1·2X** and protophanes **2·2Br**

Compound	Transition	ΔH/J g^{-1}	T_{trans}/°C	T_{cp}/°C	T_{dec}/°C
2a·2Br	LC–iso	2.6		57	
					280
2b·2Br	SC–LC	215.0	60.9		
	LC–iso			250	
					274
1a·2Br	SC–LC	21.6	162.7		
	LC–iso			255	
					309
1b·2Br	SC–LC	41.3	107.2		
					311
1b·2BF$_4$	SC–LC	30.8	113.1		
	LC–iso			200	
					325
1b·2CF$_3$SO$_3$	SC–LC$_1$	38.3	87.2		
	LC$_1$–LC$_2$	^{a}	98.6		
	LC$_2$–iso			210	
					355
1b·2(N(CF$_3$SO$_2$)$_2$)	SC–LC$_1$	51.9	96.5		
	LC$_1$–LC$_2$		106		
	LC–iso			^{b}	
					343

SC: solid crystal, LC: liquid crystal, iso: isotropic phase, T_{cp}: clearing point temperature, T_{dec}: decomposition temperature. ^{a} The peak observed was a shoulder almost overlapped to the previous one (at 87.2 °C), thus the enthalpy was overestimated. ^{b} Value could not be determined.

is driving the supramolecular order, and anion exchange allows observation of liquid crystal behaviour for the dicationic macrocycles **1b·2X** exhibiting lower transitions than **1a·2Br**. Thus, the anion was also observed to be a factor that tunes the thermal behaviour. In this case, **1b·2BF$_4$** exhibits a transition at 113.1 °C, and shows a clearing point at 200 °C (Table 2). Compound **1b·2CF$_3$SO$_3$** exhibits a SC to LC transition at 87.2 °C, and shows a clearing point at 210 °C (Table 2), and **1b·2N(CF$_3$SO$_2$)$_2$** experiences a transition at 96.5 °C detected by DSC (but not by POM) and a second transition at 106 °C (not detected by DSC) to an isotropic phase which shows a long range order, detected by XRD (see Fig. S2a in ESI†), and is therefore assigned to a cubic phase (Table 2). The clearing point of **1b·2N(CF$_3$SO$_2$)$_2$** could not be determined by POM-HS due to the absence of birefringence (see Fig. S2b in ESI†). Likewise, the transition temperature from SC to LC is in the order of Br$^-$ ≈ BF$_4^-$ > CF$_3$SO$_3^-$ ≈ [N(CF$_3$SO$_2$)$_2^-$]. These results could be caused by the significant effect that anions have on the phase transition temperature depending on anion size and lipophilicity as well as the degree of affinity between the bis-imidazolium salt and the counter-ion, as indicated by NMR spectroscopy (see Table 1). Although there is no general evidence implying which anions might favour the formation of mesophases, in the compounds described here it is clear that the bromide counter-ion leads to a very high melting point. This fact is very likely caused by the strong interaction between this anion and the macrocyclic head group, which can be observed in solution for related systems.[10] The strong interaction between the head group and counterion in the polar region of the material would be expected to lead to greater propensity for the formation of a solid.

Finally, comparison with the corresponding open chain analogues indicates that the macrocyclic structure induces crystallinity
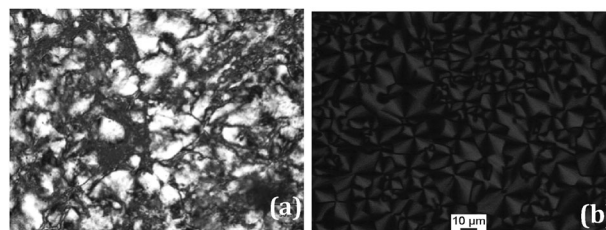

Fig. 2 POM-HS images of (a) **1b·2Br** at 26 °C, and of (b) **2a·2Br** at 27 °C.

in the dicationic scaffold. As can be seen in Table 2, the clearing, transition and decomposition temperatures are much higher for **1·2Br** than for **2·2Br**, suggesting that the cyclic framework adds more stability to the self-organised molecules, which require more energy to undergo molecular displacement and destabilization.

All of the mesophases appear to be of the smectic type (except **1b·2N(CF$_3$SO$_2$)$_2$**) as indicated by their texture in POM and/or the small angle X-ray diffractograms (Fig. S1 and S2a in ESI†). As an example, Fig. 2 shows POM-HS images of the cyclophane **1b·2Br** and the protophane **2a·2Br**. For the cyclophane **1b·2Br** a gradual melting process was observed. Images for protophane **2a·2Br** allowed the observation at room temperature of the focal conic texture characteristic of a smectic lamellar mesophase.

For those compounds with LC behaviour, variable temperature XRD experiments were carried out, and the results are shown in Table S1 in ESI.† For the bromide salts with octadecyl chains, the layer distance (d-spacing) in the LC organisation was deduced from Bragg's law ($d = 2\pi/q$) as *ca.* 2.5 nm or 4 nm. The former would appear to arise from layers in which the alkyl chains from adjacent layers interdigitate deeply, while for the latter less interpenetration of layers takes place. Remarkably, for **1b·2X** the layer distance is similar for the different anions except for **1b·2N(CF$_3$SO$_2$)$_2$**, this compound showing a considerable increase that can be attributed to a steric effect that prevents molecular interdigitation. Also, a variation of d depending on the temperature and the alkyl chain length is observed. In general, higher temperatures induce a decrease in the d value, probably as a consequence of an increase in the fluidity of the layers. However, the distance is slightly increased with the length of the hydrophobic tails. The size of the two anions of each molecule in the material surely plays a role in this variation in spacing.

This work shows that the reduced conformational flexibility at the core of these readily accessible dicationic macrocycles gives a greatly increased stability to the thermotropic mesophase when compared with the analogous open chain compounds. This effect can be considered an advantage in other soft matter systems, such as vesicles or nanoparticles, areas which we are currently exploring. In addition, since the thermotropic behaviour of the macrocyclic compounds can be modified by the counter-ion, variations in the mesophases can be modulated by anion exchange.

Experimental

Synthesis of dicationic macrocycles 1·2X

Dicationic macrocycles 1·2Br. 1,3-Bis(imidazolylmethyl)-5-alkyloxybenzene **5a** or **5b** (0.63 mmol) was stirred in dry MeCN (80 mL) at 80 °C under an argon atmosphere until dissolved (10 minutes). A solution of 1,3-bis(bromomethyl)-5-alkyloxybenzene

4a or **4b** (0.63 mmol) in dry MeCN (80 mL) at 60 °C was added. The stirring of the colourless solution was continued at 80 °C for 24 hours. The solution was cooled down to room temperature and the solvent was evaporated. The residue was washed with *n*-hexane and the white solid was filtered off to give **1a·2Br** as a white solid (0.39 g, 75%). Alternatively, CH_2Cl_2 (40 mL) was added to the residue, the white solid was filtered off, washed with CH_2Cl_2 (10 mL) and dried to obtain **1b·2Br** as a white solid (0.48 g, 72%).

Dicationic macrocycle 1b·2BF₄. A solution of ammonium tetrafluoroborate (0.004 g, 0.04 mmol) in water (0.4 mL) was added to a solution of the macrocycle **1b·2Br** (0.020 mg, 0.02 mmol) in EtOH (9 mL) at 40 °C. A white solid precipitated and the stirring was continued for 1.5 hours at room temperature. The white solid was filtered off, washed with water (5 mL), and redissolved in CH_2Cl_2. The organic solvent was dried over $MgSO_4$, filtered and the solvent was evaporated to give **1b·2BF₄** as a white solid (0.01 g, 64%).

Dicationic macrocycle 1b·2CF₃SO₃. Macrocycle **1b·2Br** (0.10 g, 0.10 mmol) was stirred in abs. EtOH (44 mL) at 55 °C until dissolved. A solution of silver trifluoromethanesulfonate (52 mg, 0.20 mmol) in abs. EtOH (5 mL) was added in the dark. A white solid precipitated and the stirring was continued for 1 hour. The solvent was evaporated and the residue was partitioned between CH_2Cl_2 (75 mL) and water (75 mL). The aqueous phase was extracted with CH_2Cl_2 (2 × 75 mL), then the organic phase was washed with water (2 × 150 mL), dried over $MgSO_4$, filtered and the solvent was evaporated to give the macrocycle **1b·2CF₃SO₃** as a grey solid (0.05 g, 47%).

Dicationic macrocycle 1b·2(N(CF₃SO₂)₂). Macrocycle **1b·2Br** (0.02 g, 0.02 mmol) was stirred in abs. EtOH (8 mL) at 50 °C until dissolved. A solution of lithium bis(trifluoromethanesulfonyl)imide (0.01 g, 0.04 mmol) in abs. EtOH (0.4 mL) was added. The stirring was continued for 1 hour at 50 °C. The solution was cooled down to room temperature and the solvent was evaporated. Water (8 ml) was added to the residue and the solid was filtered off to give the macrocycle **1b·2(N(CF₃SO₂)₂)** as a white solid (0.02 g, 56%).

LC behaviour characterization equipment

POM-HS. Reichert Polyvar 2 polarizing optical microscope from Leica with a Sony camera and a Mettler FP82 HT hot stage equipped with a Mettler FP90 central processor.

DSC. Mettler Toledo DSC 821. Software used for results evaluation: STAR SW 9.20 Software.

TGA. Mettler Toledo TGA/SDTA 851. Capsules: crucible standard of aluminium (400 µL and 100 µL, respectively) with a perforated cap. Nitrogen was used as purgative gas in all measurements.

XRD. S3 MICRO instrument (Hecus X-ray System, Graz, Austria) with point focalization, equipped with a GENIX microfocus X-ray source operating at 50 kV and 1 mA and a FOX2D point-focusing element (both from Xenocs, Grenoble). The scattered intensity was recorded using position-sensitive detectors (Hecus). For measurements, powder samples were placed in flame-sealed glass capillaries (Hilgenber. Markröhrchen, d = 1 mm, large 80 mm and thickness of 0.01 mm).

Acknowledgements

References

1 (*a*) S. Kumar, *Chem. Soc. Rev.*, 2006, **35**, 83–109; (*b*) P. Oswald and P. Pieranski, *Liquid Crystals*, CRC Press, 2006; (*c*) P. G. de Gennes and J. Prost, *The Physics of Liquid Crystals*, Oxford University Press, New York, 1993.

2 K. Binnemans, *Chem. Rev.*, 2005, **105**, 4148–4204.

3 (*a*) P. Bonhôte, A.-P. Dias, N. Papageorgiou, K. Kalyanasundaram and M. Grätzel, *Inorg. Chem.*, 1996, **35**, 1168–1178; (*b*) A. E. Bradley, C. Hardacre, J. D. Holbrey, S. Johnston, S. E. J. McMath and M. Nieuwenhuyzen, *Chem. Mater.*, 2002, **14**, 629–635; (*c*) A. Getsis and A.-V. Mudring, *Cryst. Res. Technol.*, 2008, **43**, 1187–1196; (*d*) J.-M. Suisse, L. Douce, S. Bellemin-Laponnaz, A. Maisse-François, R. Welter, Y. Miyake and Y. Shimizu, *Eur. J. Inorg. Chem.*, 2007, 3899–3905; (*e*) X. Wang, C. S. Vogel, F. W. Heinemann, P. Wasserscheid and K. Meyer, *Cryst. Growth Des.*, 2011, **11**, 1974–1988.

4 (*a*) Y.-S. Ding, M. Zha, J. Zhang and S.-S. Wang, *Colloids Surf., A*, 2007, **298**, 201–205; (*b*) J. E. Bara, E. S. Hatakeyama, B. R. Wiesenauer, X. Zeng, R. D. Noble and D. L. Gin, *Liq. Cryst.*, 2010, **37**, 1587–1599; (*c*) M. Trilla, R. Pleixats, T. Parella, C. Blanc, P. Dieudonne, Y. Guari and M. W. C. Man, *Langmuir*, 2008, **24**, 259–265; (*d*) X. Li, D. W. Bruce and J. M. Shreeve, *J. Mater. Chem.*, 2009, **19**, 8232–8238.

5 P. H. J. Kouwer and T. M. Swager, *J. Am. Chem. Soc.*, 2007, **129**, 14042–14052.

6 (*a*) K. M. Lee, Y. T. Lee and I. J. B. Lin, *J. Mater. Chem.*, 2003, **13**, 1079–1084; (*b*) W. Dobbs, L. Douce, L. Allouche, A. Louati, F. Malbosc and R. Welter, *New J. Chem.*, 2006, **30**, 528–532; (*c*) M. Yoshio, T. Ichikawa, H. Shimura, T. Kagata, A. Hamasaki, T. Mukai, H. Ohno and T. Kato, *Bull. Chem. Soc. Jpn.*, 2007, **80**, 1836–1841.

7 L. Casal-Dujat, *PhD thesis*, University of Barcelona, 2010.

8 P. Wang, C. N. Moorefield and G. R. Newkome, *Org. Lett.*, 2004, **6**, 1197–1200.

9 M. M. Murray, P. Kaszynsky, D. A. Kaisaki, W. Chang and D. A. Dougherty, *J. Am. Chem. Soc.*, 1994, **116**, 8152–8161.

10 E. Alcalde, N. Mesquida and L. Pérez-García, *Eur. J. Org. Chem.*, 2006, 3988–3996, and references therein.

11 M. Tosoni, S. Laschat and A. Baro, *Helv. Chim. Acta*, 2004, **87**, 2742–2748.

12 E. Alcalde, N. Mesquida, M. Alemany, C. Alvarez-Rúa, S. García-Granda, P. Pacheco and L. Pérez-García, *Eur. J. Org. Chem.*, 2002, 1221–1231.